



Fisheries and Oceans
Canada

Pêches et Océans
Canada

Ecosystems and
Oceans Science

Sciences des écosystèmes
et des océans

Canadian Science Advisory Secretariat (CSAS)

Research Document 2016/067

Gulf Region

Abundance indices and selectivity curves from experimental multi-panel gillnets for the southern Gulf of St. Lawrence fall herring fishery

T.J. Surette, C.H. LeBlanc, and A. Mallet

Fisheries and Oceans Canada
Science Branch
Gulf Region
P. O. Box 5030
Moncton, New Brunswick E1C 9B6

Foreword

This series documents the scientific basis for the evaluation of aquatic resources and ecosystems in Canada. As such, it addresses the issues of the day in the time frames required and the documents it contains are not intended as definitive statements on the subjects addressed but rather as progress reports on ongoing investigations.

Research documents are produced in the official language in which they are provided to the Secretariat.

Published by:

Fisheries and Oceans Canada
Canadian Science Advisory Secretariat
200 Kent Street
Ottawa ON K1A 0E6

[http://www.dfo-mpo.gc.ca/csas-sccs/
csas-sccs@dfo-mpo.gc.ca](http://www.dfo-mpo.gc.ca/csas-sccs/csas-sccs@dfo-mpo.gc.ca)



© Her Majesty the Queen in Right of Canada, 2016
ISSN 1919-5044

Correct citation for this publication:

Surette, T.J., LeBlanc, C.H., and Mallet, A. 2016. Abundance indices and selectivity curves from experimental multi-panel gillnets for the southern Gulf of St. Lawrence fall herring fishery. DFO Can. Sci. Advis. Sec. Res. Doc. 2016/067. vi + 23 p.

TABLE OF CONTENTS

| | |
|--------------------------------|----|
| LIST OF TABLES..... | IV |
| LIST OF FIGURES | IV |
| ABSTRACT..... | V |
| RÉSUMÉ | VI |
| INTRODUCTION | 1 |
| METHODS..... | 1 |
| STUDY DESIGN | 1 |
| DATA ISSUES | 2 |
| MISSING SOAK TIMES | 3 |
| GILLNET SELECTIVITY MODEL..... | 3 |
| MODEL DESCRIPTION | 3 |
| SELECTIVITY-AT-AGE..... | 4 |
| RESULTS | 5 |
| DISCUSSION..... | 6 |
| UNCERTAINTIES | 7 |
| SAMPLING RECOMMENDATIONS..... | 8 |
| CONCLUSION..... | 8 |
| ACKNOWLEDGEMENTS | 8 |
| REFERENCES CITED..... | 9 |
| TABLES..... | 10 |
| FIGURES..... | 13 |

LIST OF TABLES

| | |
|---|----|
| Table 1. Number of experimental net sets by year and region..... | 10 |
| Table 2. Number of samples of Atlantic herring collected by region, year and individual mesh sizes of the experimental gillnets from the fall Atlantic herring fishery of the southern Gulf of St. Lawrence. | 11 |
| Table 3. Models fitted to the experimental gillnet data. Shown are the parameter values, log-likelihood values, number of parameters (k), and AIC values. | 12 |

LIST OF FIGURES

| | |
|---|----|
| Figure 1. Map of experimental net fishing locations (n = 236) from logbook entries. The Pictou and Fisherman’s Bank spawning areas were grouped in the South region, the Escuminac and West PEI areas into the Middle region and the Miscou into the North region. | 13 |
| Figure 2. Number of experimental net samples per day (starting from August 1st) by region and year. Grey squares indicate one sample and black squares indicate that two fishermen were active. | 14 |
| Figure 3. Ratio of sample weight to fisherman-estimated catch weight versus catch weight. The dashed line shows the theoretical sampling ratio under the prescribed fishing and sampling protocol..... | 15 |
| Figure 4. Histogram of reported experimental net soak times from logbooks. | 16 |
| Figure 7. Fitted gamma-type selectivity curves by mesh size for the inference model based on the negative binomial with constant fishing power. | 19 |
| Figure 8. Proportions-at-length of Atlantic herring for each mesh size, as estimated from the inference model (solid line) and the model where fishing power of each panel is proportional to mesh size (dashed lines). | 20 |
| Figure 9. Standardized observed counts versus predicted mean counts from the inference model..... | 21 |
| Figure 10. Catch-at-length index by year and region as inferred from the gillnet selectivity model. Circle areas are proportional to the estimated mean standardized catch, in numbers per hour. | 22 |
| Figure 11. Bubble plot of catch-at-age estimates from the inference model by year and region. Circle areas are proportional to the estimated mean standardized catch, in numbers per hour. | 23 |

ABSTRACT

In partnership with Fisheries and Oceans Canada (DFO), fish harvesters participating in the Atlantic herring (*Clupea harengus*) fall fishery in NAFO 4T surveyed five spawning grounds in the southern Gulf of St. Lawrence using multi-panel experimental gillnets over the course of their regular fishing activities from 2002 to 2013. The results of these surveys are analyzed to identify whether they can be used as indices of local abundance for assessment of fall 4T herring. Catches were analyzed with a selectivity model, which produced mesh-specific selectivity curves, length-based population indices, and age disaggregated indices for the North, Middle, and South regions of the southern Gulf of St. Lawrence. The selectivity model has little ability to estimate how fishing power varies with mesh size, so population indices might be length-biased. Uncertainties also underlie the scale of catches due to methodological and biological differences between years and regions. Nevertheless, cohort tracks in the catch-at-age were fairly consistent between regions and indicate that some dynamics of the underlying population are captured. Consequently, the selectivity and catch-at-age indices were approved for use in future population dynamics models of Atlantic herring for the southern Gulf of St. Lawrence.

Indices d'abondance et courbes de sélectivité issus de la pêche aux filets maillants expérimentaux à panneaux multiples du hareng d'automne dans le sud du golfe du Saint-Laurent

RÉSUMÉ

En partenariat avec Pêches et Océans Canada, les pêcheurs participant à la pêche d'automne du hareng de l'Atlantique (*Clupea harengus*) dans la division 4T de l'OPANO ont effectué des relevés dans cinq frayères du sud du golfe du Saint-Laurent en utilisant des filets maillants expérimentaux à panneaux multiples pendant leurs activités de pêche courantes entre 2002 et 2013. On procède à l'analyse de ces relevés pour déterminer s'ils peuvent servir d'indices de l'abondance locale pour l'évaluation du hareng d'automne dans la division 4T. Les prises ont été analysées à l'aide d'un modèle de sélectivité duquel sont issues des courbes de sélectivité propres au filet, des indices de l'abondance selon la longueur et des indices des prises selon l'âge pour les régions du nord, du centre et du sud du golfe du Saint-Laurent. Le modèle de sélectivité est peu efficace pour estimer l'influence du maillage sur la capacité de pêche, de sorte que la longueur des prises peut fausser les indices de population. Par ailleurs, il y a des incertitudes entourant l'ampleur des prises à cause des variations des méthodes et des éléments biologiques d'une année à l'autre et d'une région à l'autre. Néanmoins, les suivis de cohortes à partir des prises selon l'âge affichent des résultats assez uniformes d'une région à l'autre et laissent croire que certains aspects de la dynamique des populations ont été saisis. C'est pourquoi les indices de sélectivité et de prises selon l'âge ont été approuvés pour servir éventuellement dans les modèles de dynamique des populations du hareng de l'Atlantique dans le sud du golfe du Saint-Laurent.

INTRODUCTION

The stock assessment for the southern Gulf of St. Lawrence (sGSL) fall herring stock to 2014 used a population model for all spawning grounds combined (LeBlanc et al. 2015) and management provides Total Allowable Catch (TAC) advice based on the overall sGSL biomass. The indices for this population model have includes an annual commercial gillnet catch-per-unit-effort (CPUE) index and an annual fisheries-independent acoustic survey index. There are concerns that gillnet CPUE does not track population biomass well, because fisheries that target spawning aggregations often exhibit hyperstability, where CPUEs remain elevated even as stock abundance declines (Erisman et al. 2011). Furthermore, there is a risk of bias in the assessment of only including information obtained for large scale processes when fisheries occur on discrete spawning grounds, as is the case with the sGSL commercial gillnet fishery for Atlantic herring.

From 2002 to 2013, experimental gillnets, consisting of multiple panels of varying mesh size, were used by commercial fish harvesters participating in a hydro-acoustic study on the five major Atlantic herring fall spawning areas located within the coastal waters of the sGSL; Miscou and Escuminac-Richibucto, N.B., Fisherman's Bank and West PEI, P.E.I., and Pictou, N.S. (LeBlanc 2013) (Fig. 1). These catches were used to calibrate the signal strength in order to obtain nightly estimates of spawning biomass in various regions. These modified gillnets catch a wide range of fish sizes and provide information on the relative selectivity of various mesh sizes. In this paper, we reconstruct population length-frequencies from catches arising from multiple mesh sizes. From these, we derive a fishery-independent abundance index and derive catch-at-age estimates in combination with age sampling data.

METHODS

STUDY DESIGN

Fish harvesters from each of the five spawning grounds in sGSL (Fig. 1) were contracted to gather information during the fall fishery (LeBlanc 2013). Vessels were equipped with acoustic sonar and were charged with characterizing schools of spawning herring (LeBlanc 2013). In parallel, they deployed specially designed multi-mesh experimental gillnets. Each experimental gillnet had five panels, each with a different mesh size, from a set of seven possible mesh sizes, ranging from 2" to 2³/₄" in 1/₈" increments. All gillnets had panels with mesh sizes of 2¹/₂", 2⁵/₈" and 2³/₄" plus two of the smaller mesh sizes which varied among fish harvesters. The gillnet specifications were provided to participating fish harvesters by DFO.

The protocol for the fishing operations was:

- fished a minimum of once per week,
- set as stand-alone nets,
- set for a target soak of 1 hour though actually soak times were recorded, and
- set on the spawning grounds during the commercial fishery.

Fish harvesters were provided with logbooks in which to record the date of fishing, the location of the net set, the soak time, the estimated catch in weight per mesh size, and other comments. Catch weights per panel are estimated by fishermen onboard the vessel. For each panel/mesh size, catches up to a full crate (~120 lbs) were retained for sampling while larger catches were sub-sampled. Length-frequencies were obtained from crates for each experimental mesh size. A subset of herring (two fish per 0.5 cm) were brought to the lab for complete biological

sampling, including individual length, weight, sex, maturity, gonad weight, age, and spawning season.

The regularity at which nets were set varied according to weather condition, fishery closures, and equipment malfunctions. Fish harvesters were allowed to fish after the quota had been attained because the length of the acoustic surveys extended to 28 days regardless of the fishing season (LeBlanc 2013).

The data used for the following analyses were extracted from experimental gillnet survey logbook data entries, length-frequencies, and age data from panel-specific catch samples for the period 2002 to 2013. Spawning grounds were grouped into three regions: North (Miscou), Middle (Escuminac and West PEI) and South (Pictou and Fisherman’s Bank). Fishing locations as recorded in logbooks are shown in Figure 1. A total of 236 sets were considered over the study period (Tables 1). The frequency of net sets over the fishing season is shown in Figure 2.

DATA ISSUES

There were a number of issues with these data. Recorded latitude and longitude coordinates for each set are plotted in Figure 1. Thirteen sets had no recoverable fishing coordinates. However, since the interest was in analyses by fishing region, the geographical provenance of catches could be determined either by coordinates or landed port. Only samples from within the five spawning regions were kept for the analysis.

Gillnet mesh sizes were sometimes misidentified. Mesh sizes were corrected so as to respect temporal continuity. In other words, fish harvesters tended to use the same nets from year to year, so missing or misidentified mesh sizes were inferred from adjoining years. Where it was not possible to infer the mesh size, the corresponding records were deleted.

Length-frequency and age sample data were linked to particular logbook entries using landed dates, home port information, vessel identifiers and mesh sizes. Cases where length or age samples could not be matched with reasonable certainty to a corresponding logbook entry were discarded (fewer than 10 sets). A total of 97,149 fish were sampled for length and 19,369 fish were aged from both the experimental study and fall commercial sampling. There were 42 instances of gillnet panels with recorded catches but having no associated length-frequency or age samples. The catches of these samples were taken into account when calculating the mean length-frequency by year and region (see below). A total of 970 length-frequency samples were retained for this analysis.

Catch weights for each gillnet panel were estimated by fish harvesters. Where the entire catch was sampled, i.e., where estimated catch weights were 120 lbs or less, an improved catch weight estimate was derived using an allometric length-weight relationship:

$$w = 4.97 \cdot 10^{-3} \cdot l^{3.17} \tag{1}$$

where l is the length of fish in cm and w is the weight in grams. This equation was estimated using the laboratory measured length and weight measurements ($n = 32,337$) from the experimental gillnet study. A multiplicative log-normal error term was assumed. A comparative plot of the ratio between derived sample weight and the harvester-estimated catch weight is shown in Figure 4, showing a high degree of variability. For catches larger than 120 lbs, the estimate provided by the fisherman was used. While the variation about the sample versus observed catch weights is significant, we note that for weights under 120 lbs, the ratio between the two is centered on 1 and so estimates do not seem to be biased overall. Ratios for larger catches show less variation and was generally lower than the reference line prescribed by the

sampling protocol (Fig. 3). There were four instances where catch weights were not recorded and these were assumed to be zero.

Two samples from Miscou (October 19 and October 26 in 2004) were removed from the analysis owing to the lateness of the fishing dates. If we consider that each set had five separate catches, one for each panel, a total of 168 catches were nil out of the 1,180 sets. The number of catches sampled by year, region and mesh size is presented in Table 2.

MISSING SOAK TIMES

Soak times are required for standardizing the total number of fish caught per set. However, there were 10 sets (in 2004, 2005 and 2008), generally with null or low catches, for which there was no recorded soak time. While the protocol called for a soak time of one hour, reported values ranged from 10 minutes to 10 hours (Fig.4). Soak times were often recorded to the nearest hour or half-hour increment. In cases where catches were the result of multiple sets, soak times were simply summed into a single value.

To infer missing soak-times, a Bayesian hierarchical model was constructed to predict soak time by year and vessel captain. This model had the following structure:

$$\ln \mu_{ij} = \delta + \alpha_i + \beta_j + (\alpha\beta)_{ij} + \varepsilon_{ij} \quad (2)$$

where $\alpha_i \sim N(0, \sigma_\alpha^2)$, $\beta_j \sim N(0, \sigma_\beta^2)$, $(\alpha\beta)_{ij} \sim N(0, \sigma_{\alpha\beta}^2)$, and $\varepsilon_{ij} \sim N(0, \sigma_\varepsilon^2)$ are hierarchical priors for year effects, captain effects, year by captain interaction effects and residual error, respectively. The intercept parameter, $\delta \sim N(0, 10^6)$, and the variance parameters $\sigma_*^2 \sim \text{Gam}(10^{-4}, 10^{-4})$ were given diffuse non-informative priors. MCMC simulations were performed using OpenBUGS 3.2.2 (Lunn et al. 2000) and posterior means for each missing soak time were then predicted and substituted for the missing data.

GILLNET SELECTIVITY MODEL

Observed sample length-frequencies were first standardized to a one hour soak time, then scaled by the sampling ratio. An average length-frequency by year, region and mesh size for sampled sets was then obtained by using catch weights as weighting factors. For year, region and mesh size combinations containing un-sampled catches, the average of the observed length-frequencies were first converted to proportions-at-length, and then multiplied by the average of all catch weights. The resulting group length-frequencies served as inputs to the gillnet selectivity model. Figure 5 shows the mean standardized length-frequencies for each panel mesh size, averaged over year and region.

MODEL DESCRIPTION

The following gillnet selectivity model, following Millar and Holst (1997), was applied to the standardized and averaged length-frequency data by year, region and mesh size. Group means have a log-linear form:

$$\ln \mu_{ijkl} = \log(p_k) + \log(\lambda_{ijl}) + \log(s_k(L_l)) \quad (3)$$

where μ_{ijk} is the predicted mean for year i , region j , mesh size k and fish length index l . The relative fishing power of each mesh size is expressed through p_k , the selectivity curves by mesh and fish length are $s_k(L_l)$ and the relative abundance of the underlying population by year and region λ_{ijl} , which is the main quantity of interest.

Two count distributions, the Poisson and the negative binomial, were considered as error models. Continuous variants of the likelihood functions of these count models were used, since the input data were generally non-integer, owing to the averaging, standardizing and rescaling operations which were applied. To facilitate inference, a negative binomial parameterized by its mean μ was used:

$$P[X = x] = \left(\frac{r}{r+\mu}\right)^r \frac{\Gamma(r+x)}{\Gamma(x+1)\Gamma(r)} \left(\frac{\mu}{r+\mu}\right)^x \quad (4)$$

where μ is defined by log-linear equation (3), x are the average counts, and r is a precision parameter which controls the overall dispersion of the distribution.

Two types of selectivity curves were considered, the Gaussian type and the gamma-type, which are scaled versions of their probability density analogues, with peak values at their respective modes set to 1. The relative fishing power of the net panels was either assumed to be $p_k = 1$, for all values of k or allowed to vary by mesh size (i.e., treated as a factor). The model assumes geometric similarity between fish and mesh sizes, i.e., that the location of their modal values as well as their spreads of the selectivity curves be proportional to mesh size.

The Gaussian-type selectivity curve is defined given by:

$$s_k(L) = \exp\left\{-\frac{(L-\phi_1 m_k)^2}{2(\phi_2 m_k)^2}\right\} \quad (5)$$

while the gamma-type selectivity curve had the form:

$$s_k(L) = \left(\frac{L}{(\alpha-1)\phi m_k}\right)^{\alpha-1} \exp\left(\alpha - 1 - \frac{L}{\phi m_k}\right) \quad (6)$$

where L corresponds to fish length (in cm), k is an index of mesh size, m_k is mesh size k (in inches), α is the gamma distribution shape parameter and ϕ is a scale parameter. The mode of the gamma curve is given by $(\alpha - 1)\phi m_k$. Given that the value of both selectivity models at their modal size is 1, the relative selectivity is given by p_k . When $p_k = 1$, the population estimate and the mean coincide, $\lambda_{ijl} = \mu_{ijkl}$ at this modal size.

In total, five different models were considered for the analysis. There were two Poisson and two negative binomial models, each with a combination of either Gaussian or Gamma selectivity curves (four models) under constant fishing power $p_k = 1$. The fifth model considered was a negative binomial model with a Gamma-type selectivity curve with variable fishing power parameters p_k .

Length categories with zero frequencies, i.e., null catches, within a particular year and region do not contribute to the likelihood and were removed from the analysis. The total number of standardized count observations, by year, region, and mesh size and fish length was 4,266. Maximum likelihood solutions for these models were obtained iteratively using the BFGS quasi-Newton method within the *optim* function from the **R** *stats* package (R Core Team, 2013).

Catch-at-age estimates were calculated from age-length keys constructed from both the experimental and commercial gillnet age samples, separated by region.

SELECTIVITY-AT-AGE

While it may be reasonably assumed that selectivity-at-length has not changed through time, variations in growth (i.e., size-at-age) imply variation in selectivity-at-age. Catch-at-age estimates may be standardized for changes in growth either by applying the length-selectivity

curve on length-frequency data prior to applying age-length keys, or by applying the age-selectivity values, which are a combination of time-invariant length-selectivity curves and time-varying age-length keys. For each year, or for each group wherein growth can be assumed to be homogeneous, the calculation of selectivity at age a , denoted $s(a)$ proceeds as follows.

Summing over lengths l , the selectivity-at-length, denoted $s(l)$, is multiplied with the length distribution at-age, denoted $p(l|a)$. This value is derived from the joint length-age distribution $p(l, a)$, which is in turn obtained from the age-length key $p(a|l)$ applied to an estimate of population length distribution $p(l)$. Mathematically, this is expressed as:

$$\begin{aligned}
 s(a) &= \sum_l s(l) \times p(l|a) \\
 &= \sum_l s(l) \times \frac{p(l,a)}{p(a)} \\
 &= \sum_l s(l) \times \frac{p(a|l)p(l)}{p(a)} \\
 &= \frac{1}{p(a)} \sum_l s(l) \times p(a|l) \times p(l)
 \end{aligned}$$

The fall commercial CPUE index for herring was adjusted for time-varying age-selectivity using the above procedure. Annual age-length keys were calculated from combined otolith samples from the present study along with commercial fishery samples. Annual population distributions were calculated from the experimental and commercial gillnet fishery length samples. The resulting selectivity-at-age values were used as scaling coefficients with the fishery catchability component of the population dynamics model.

RESULTS

Maximum likelihood parameter estimates for each of the five fitted models, along with corresponding log-likelihood and AIC values are shown in Table 3. The model with the lowest AIC value (11,545.1) was the negative binomial with gamma-type selectivity and variable fishing power. However, the estimated fishing power values were deemed to vary unrealistically with mesh size, as a more monotone pattern would be expected. The fitted selectivity curves for this model are shown in Figure 6. As a consequence, the negative binomial model with gamma-type selectivity was chosen as the inference model, with an AIC value of 11,923.6. The maximum likelihood parameter estimates are $\hat{\alpha} = 111.49$ and $\hat{\phi} = 0.1141$. The negative binomial precision parameter was estimated to be $\hat{r} = 8.460$. The fitted gamma-type selectivity curves for this model are shown in Figure 7. Estimated modal selectivity sizes, i.e. the fish sizes which are maximally caught by each mesh, were estimated at 25.2 cm (2" mesh), 26.8 cm (2¹/₈" mesh), 28.3 cm (2¹/₄" mesh), 29.9 cm (2³/₈" mesh), 31.5 cm (2¹/₂" mesh), 33.1 cm (2⁵/₈" mesh) and 34.6 cm (2³/₄" mesh).

The selectivity model has a limited capacity for inferring the relative fishing power between gillnets of different mesh sizes. For a given fish length, the likelihood is invariant to any transformation which leaves the relative selectivity between meshes, the proportions of the underlying population abundance assigned to each panel mesh, unchanged. To see this, recall the log-linear form of the mesh selectivity model in equation (3) and assume that the selectivities for each mesh k is scaled by some constant c_l which varies by fish length class l . This yields:

$$\begin{aligned}
 \ln \mu_{ijkl} &= \log(p_k) + \log(\lambda_{ijl}) + \log(c_l s_k(L_l)) \\
 &= \log(p_k) + \log(\lambda_{ijl}) + \log(c_l) + \log(s_k(L_l))
 \end{aligned}$$

$$= \log(p_k) + \log(c_l \lambda_{ijl}) + \log(s_k(L_l))$$

$$= \log(p_k) + \log(\lambda'_{ijl}) + \log(s_k(L_l))$$

which is simply the original model from equation (3), except all population abundances for length class l , will have maximum likelihood estimates (MLEs) for population abundances which are $\lambda_{ijl} = \lambda'_{ijl}/c_l$, where λ_{ijl} are the MLEs from the original model. We see that the group means, and thus the likelihood, are left unchanged.

If we assume that fishing power in the inference model scales linearly with mesh size, we obtain a model fit with negligible change in likelihood, less than a 0.1 difference. While the relative increase in fishing power between 2" and 2³/₄" gillnets for this modified model is 37.5%, the relative proportion between gillnets changes minimally, as shown in Figure 8, which is the reason the likelihood changes so little.

A scatterplot of predicted mean versus empirical mean values of standardized catches by year, region, and mesh size and fish length is shown in Figure 9. There appears to be no bias between predicted and the empirical values.

Population length-frequency estimates from the inference model by year and region are shown in Figure 10. Some trends are visible in the estimates, notably an increasing trend, probably due to a recruitment pulse, from 2003 to 2006 across the three regions. Such cohort trends are somewhat visible from 2009 to 2013 across regions. Some estimates seem to be out of step with observed trends, such as the 2007 and 2010 estimates for the Middle region. In this case, the participating fisherman from Escuminac was inactive and thus catches for the Middle region were only represented by the participating fisherman from West PEI, whose catches were ostensibly lower.

Catch-at-age estimates by year and region are shown in Figure 11. These were obtained by applying age-length keys by year and region to length-frequencies from the model output. Age-length keys were constructed from combined age samples from both experimental and commercial gillnet catches. Cohort tracks are visible in each region, confirming recruitment pulses observed in length-estimated frequencies. The 1998 to 2001 year-classes were relatively strong in the Middle and South regions, with weaker pulses in the North region. Though somewhat more variable, the 2004 and 2005 year-classes were associated with stronger recruitment in all three regions.

DISCUSSION

Experimental multi-panel gillnet data were used to calculate indices of population age distribution for fall spawning Atlantic herring. Maximum likelihood was used to fit a negative binomial model, which accounts for over-dispersion in the count data. While there were a number of data issues, such as missing or inaccurate data, these were corrected prior to the analysis, using either formal inference models (e.g., missing soak times, sample catch corrections) or reasonable suppositions.

Selectivity curves were also produced as output from the model for each mesh size. These curves are useful for standardizing other types of gillnet catch data. For instance, where the commercial fishery gear choice varies over time, if the changes in gear are known, then length-selectivity curves can be used to convert catch-at-length estimates to the scale of a reference mesh size or to the local fishable population. Similarly, it was shown how selectivity curves and length-age data may be combined to standardize gillnet catch-at-age estimates where changes in growth may have changed through time.

Catch-at-age estimates derived from the model output showed cohort tracks and recruitment pulses which were mostly consistent among regions.

Among the conditions required for the index to be valid, experimental gillnet catches are required to be some fixed proportion of the abundance of each spawning aggregation. Violations of this assumption are permitted, so long as the expected value of catches respects the proportionality, which is assumed constant across year and region. Compliance with the assumption will depend on geometrical considerations such as the complexity of the local spatial distribution of the aggregations, how the distribution scales with abundance of fish, as well as where experimental gillnets are placed over the aggregations.

UNCERTAINTIES

The selectivity model has a limited capacity for inferring the relative fishing power between gillnets of different mesh sizes, an issue previously discussed by Millar (1995) and Millar and Holst (1997). While there is some empirical evidence that fishing power should be scaled with mesh size in some specialized studies (Borgstrom 1989), it cannot be inferred from our data, as the likelihood in our case is insensitive to this assumption. Whether the assumption of constant fishing power across mesh sizes is reasonable for Atlantic herring is unknown, however it may be reasonable given the similarities of net material, positioning, layout, and geometries.

The other goal of this experimental gillnet study was to estimate catch-at-age indices of fall spawning stocks in each of the three regions by year. To be useful, these indices need to be comparable between years within regions and ideally between regions. Fish harvesters were directed to fish over the denser parts of the aggregation, as identified by acoustic sounders. Following this directive may be complicated by the dynamics of the fishing fleet, which may sometimes limit access to richer fish densities, as well as the movement of the herring schools themselves. For the model, we assume that fishermen-specific factors, such as differences in fishing technique, are negligible between participating fish harvesters.

There were also issues with the precision of observed catches, given that panel catch weights were estimated by fish harvesters rather than weighed. Comparison of these estimated weights with those estimated from length-frequency samples, while unbiased on average, revealed substantial variability, often exceeding a 50% level of error. In addition, soak time also seems to have been approximated in many instances, as soak times were often recorded to the nearest hour or half-hour period. Catch rates, being the combination of these two values, may thus contain high levels of observation error. This level of error probably varies among fish harvesters, depending on the level of rigor applied by each participant.

Some regions have spawning aggregations which are more tightly concentrated than others, and correspondingly fleets behave in a more concerted manner in some regions than others. There is a high probability that some spawning aggregations were not fished by participating fish harvesters. This may occur either because they were undetected or exploited by other portions of the fishing fleet. Unfished aggregations are unaccounted for in the current study, and variations in their number and size by year or region would pose serious violations of the proportionality assumption.

The temporal distribution of samples may also produce biases. Herring fishing activity is dependent on incoming spawning aggregations. Activity of participating fish harvesters is inherently linked to the activity of the fleet. The abundance index produced is thus not linked to the average abundance over the season, but rather the abundance when the fishing fleet is active. Thus annual or regional variations in fleet activity, such as weekend closures, attainment of quotas, and market prices, will influence the behaviour of participating fish harvesters. Sampling effort also varied temporally.

SAMPLING RECOMMENDATIONS

Some simple sampling recommendations for future iterations of this study include:

- Recording total and sample catch weight in the logbooks.
- Recording the total number of un-sampled fish would also improve accuracy of panel gillnet catches.
- Strict adherence to the experimental protocol particularly; nets should be set within the spawning aggregation, an accurate measure of soak time, properly identified mesh sizes in logbooks, experimental gillnets are to be set alongside, but not attached to, their regular fishing gear.

CONCLUSION

Despite numerous underlying uncertainties, the presence of cohort tracks in catch-at-age estimates indicates that age and length-frequency samples are tracking some of the dynamics of the underlying population. While there is uncertainty as to the scale of catches, length-frequency samples, age-length keys and resulting catch-at-age estimates may be fairly representative of the underlying spawning stock proportions-at-length and proportions-at-age distributions. These proportions also seem consistent through time, as well as between regions, implying that there are some common patterns across sGSL herring stocks. Whereas the proportions of various length and age categories seem to have some degree of validity, the scale of the indices requires some validation. This might be achieved by comparing the nightly standardized catches with nightly biomass estimates from the concurrent acoustic spawning bed study or by inspection of residual patterns from a population model.

Despite the uncertainties in the data and analysis it was decided at the Herring Framework in April 2015 that the selectivity and catch-at-age indices were valid and could be incorporated into the future population dynamics models for sGSL herring.

ACKNOWLEDGEMENTS

This research was supported by funding from DFO Collaborative Programs. We would like to thank the Maritime Fishermen's Union and the Prince Edward Island Fishermen's Association for their collaboration, as well as the participating Fishermen, Barry Sutherland, François Beaudin, Terry Carter, Stephen Gaudet, Yvon Gionet, Kenneth Leclair, Paul-Aimé Mallet, Thang Tran, Gilles Ward, and Mark Williston.

REFERENCES CITED

- Borgstrom, R. 1989. Direct estimation of gillnet selectivity for roach (*Rutilus rutilus* L.) in a small lake. *Fish. Res.* 7: 289-298.
- Erismann, B.E., Allen L.G., Claisse, J.T., Pondella II, D.J., Miller, E.F., and Murray, J.H. 2011. The illusion of plenty: hyperstability masks collapses in two recreational fisheries that target fish spawning aggregations. *Can. J. Fish. Aquat. Sci.* 68: 1705-1716.
- Grégoire, F., and Lefebvre, L. 2003. Estimation of gillnet selectivity for Atlantic herring (*Clupea harengus harengus* L.) from the west coast of Newfoundland, 1997-2001. *Can. Industry Rep. Fish. Aquat. Sci.* no. 272.
- LeBlanc, C.H. 2013. Nightly biomass estimates from acoustic data collected during the 2002 to 2012 herring gillnet fishing activities on fall spawning aggregations in the southern Gulf of St. Lawrence. *Can. Tech. Rep. Fish. Aquat. Sci.* 3040: vi + 20 p.
- LeBlanc, C.H., Mallet, A., Surette, T., and Swain, D. 2015. Assessment of the NAFO Division 4T southern Gulf of St. Lawrence herring stocks in 2013. *DFO Can. Sci. Advis. Sec. Res. Doc.* 2015/025. vi + 142 p.
- Millar, R.B. 1995. The functional form of hook and gillnet selection curves cannot be determined from comparative catch data alone. *Can. J. Fish. Aquat. Sci.* 52: 883-891.
- Millar, R.B., and Holst, R. 1997. Estimation of gillnet and hook selectivity using log-linear models. *ICES J. Mar. Sci.* 54: 471:477.
- Poulsen, S., Nielsen, J.R., Holst, R., and Staehr, K.-J. 2000. An Atlantic herring (*Clupea harengus*) size selection model for experimental gill nets used in the Sound (ICES Subdivision 23). *Can. J. Fish. Aquat. Sci.* 57: 155-1561.
- R Core Team. 2013. [R: A language and environment for statistical computing](#). R Foundation for Statistical Computing, Vienna, Austria.
- Surette, T., LeBlanc, C.H., Claytor, R.R., and Loots, C. 2015. Using inshore fishery acoustic data on Atlantic herring (*Clupea harengus*) spawning aggregations to derive annual stock abundance indices. *Fish. Res.* 164: 266–277.

TABLES

Table 1. Number of experimental net sets by year and region.

| Year | North | Middle | South | Total |
|------|-------|--------|-------|-------|
| 2002 | 4 | 0 | 8 | 12 |
| 2003 | 7 | 8 | 16 | 31 |
| 2004 | 7 | 9 | 9 | 25 |
| 2005 | 5 | 11 | 10 | 26 |
| 2006 | 2 | 8 | 9 | 19 |
| 2007 | 3 | 4 | 9 | 16 |
| 2008 | 6 | 6 | 11 | 23 |
| 2009 | 4 | 10 | 5 | 19 |
| 2010 | 4 | 6 | 6 | 16 |
| 2011 | 5 | 7 | 7 | 19 |
| 2012 | 0 | 7 | 7 | 14 |
| 2013 | 2 | 6 | 8 | 16 |

Table 2. Number of samples of Atlantic herring collected by region, year and individual mesh sizes of the experimental gillnets from the fall Atlantic herring fishery of the southern Gulf of St. Lawrence.

| Region | Year | Gillnet mesh size (inches) | | | | | | |
|--------|------|----------------------------|-------------------------------|-------------------------------|-------------------------------|-------------------------------|-------------------------------|-------------------------------|
| | | 2 | 2 ¹ / ₈ | 2 ¹ / ₄ | 2 ³ / ₈ | 2 ¹ / ₂ | 2 ⁵ / ₈ | 2 ³ / ₄ |
| North | 2002 | na | 4 | 4 | na | 4 | 4 | 4 |
| North | 2003 | 3 | 4 | 7 | na | 7 | 7 | 7 |
| North | 2004 | 3 | 4 | 7 | na | 7 | 7 | 7 |
| North | 2005 | 1 | 4 | 5 | na | 5 | 5 | 5 |
| North | 2006 | na | 2 | 2 | na | 2 | 2 | 2 |
| North | 2007 | 3 | na | 3 | na | 3 | 3 | 3 |
| North | 2008 | 6 | na | 6 | na | 6 | 6 | 6 |
| North | 2009 | 4 | na | 4 | na | 4 | 4 | 4 |
| North | 2010 | 4 | na | 4 | na | 4 | 4 | 4 |
| North | 2011 | 5 | na | 5 | na | 5 | 5 | 5 |
| North | 2012 | na | na | na | na | na | na | na |
| North | 2013 | 2 | na | 2 | na | 2 | 2 | 2 |
| Middle | 2002 | na | na | na | na | na | na | na |
| Middle | 2003 | 8 | na | 8 | na | 8 | 8 | 8 |
| Middle | 2004 | 9 | na | 9 | na | 9 | 9 | 9 |
| Middle | 2005 | 11 | na | 11 | na | 11 | 11 | 11 |
| Middle | 2006 | 8 | na | 8 | na | 8 | 8 | 8 |
| Middle | 2007 | 4 | na | 4 | na | 4 | 4 | 4 |
| Middle | 2008 | 6 | na | 6 | na | 6 | 6 | 6 |
| Middle | 2009 | 10 | na | 10 | na | 10 | 10 | 10 |
| Middle | 2010 | 6 | na | 6 | na | 6 | 6 | 6 |
| Middle | 2011 | 7 | na | 7 | na | 7 | 7 | 7 |
| Middle | 2012 | 7 | na | 7 | na | 7 | 7 | 7 |
| Middle | 2013 | 6 | na | 6 | na | 6 | 6 | 6 |
| South | 2002 | 5 | na | 8 | 3 | 8 | 8 | 8 |
| South | 2003 | 16 | na | 16 | na | 16 | 16 | 16 |
| South | 2004 | 9 | na | 9 | na | 9 | 9 | 9 |
| South | 2005 | 10 | na | 10 | na | 10 | 10 | 10 |
| South | 2006 | 9 | na | 9 | na | 9 | 9 | 9 |
| South | 2007 | 9 | na | 9 | na | 9 | 9 | 9 |
| South | 2008 | 7 | na | 11 | 4 | 11 | 11 | 11 |
| South | 2009 | 3 | na | 5 | 2 | 5 | 5 | 5 |
| South | 2010 | 3 | na | 6 | 3 | 6 | 6 | 6 |
| South | 2011 | 3 | na | 7 | 4 | 7 | 7 | 7 |
| South | 2012 | 3 | na | 7 | 4 | 7 | 7 | 7 |

Table 3. Models fitted to the experimental gillnet data. Shown are the parameter values, log-likelihood values, number of parameters (k), and AIC values.

| Model | Distribution | Selectivity | Power | Parameters | $\log L(\hat{\theta})$ | k | AIC |
|-------|--------------|-------------|----------|---|------------------------|-----|---------|
| 1 | Poisson | Gaussian | fixed | $(\hat{\phi}_1, \hat{\phi}_2) = (12.68, 1.197)$ | -5809.1 | 810 | 12430.3 |
| 2 | Poisson | Gamma | fixed | $(\hat{\alpha}, \hat{\phi}) = (108.4, 0.117)$ | -5759.4 | 810 | 12330.8 |
| 3 | Neg.Bin. | Gaussian | fixed | $(\hat{\phi}_1, \hat{\phi}_2, \hat{r})$ $= (12.70, 1.180, 8.01)$ | -5588.5 | 811 | 11990.9 |
| 4 | Neg.Bin. | Gamma | fixed | $(\hat{\alpha}, \hat{\phi}, \hat{r})$ $= (111.5, 0.114, 8.49)$ | -5554.8 | 811 | 11923.6 |
| 5 | Neg.Bin. | Gamma | variable | $(\hat{\alpha}, \hat{\phi}, \hat{r})$ $= (127.8, 0.100, 14.45)$ | -5359.5 | 817 | 11545.1 |

FIGURES

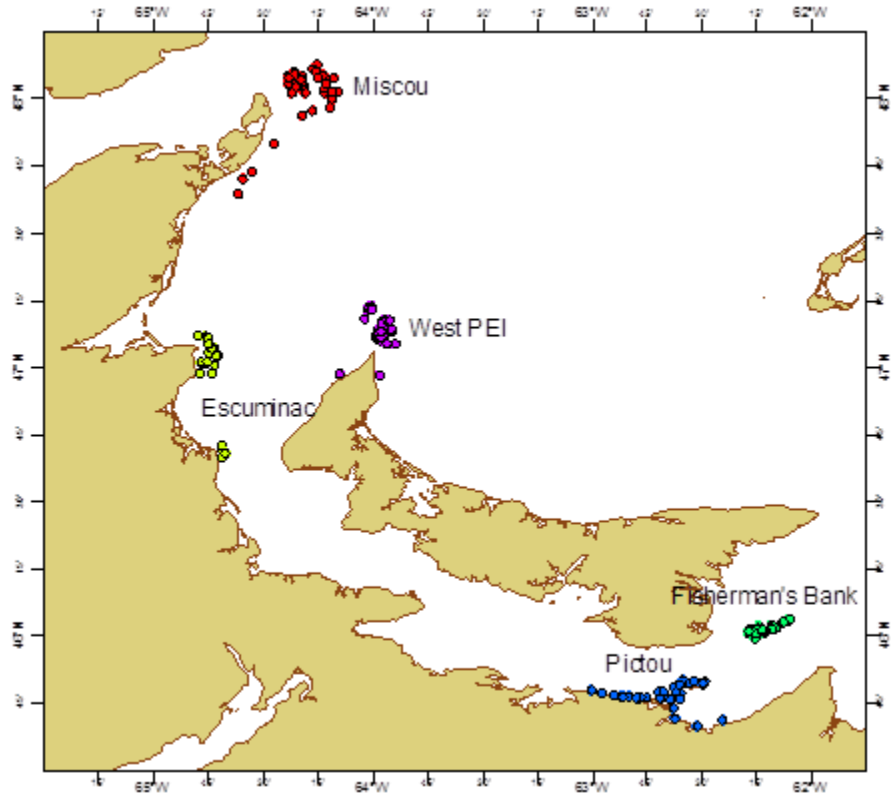


Figure 1. Map of experimental net fishing locations ($n = 236$) from logbook entries. The Pictou and Fisherman's Bank spawning areas were grouped in the South region, the Escuminac and West PEI areas into the Middle region and the Miscou into the North region.

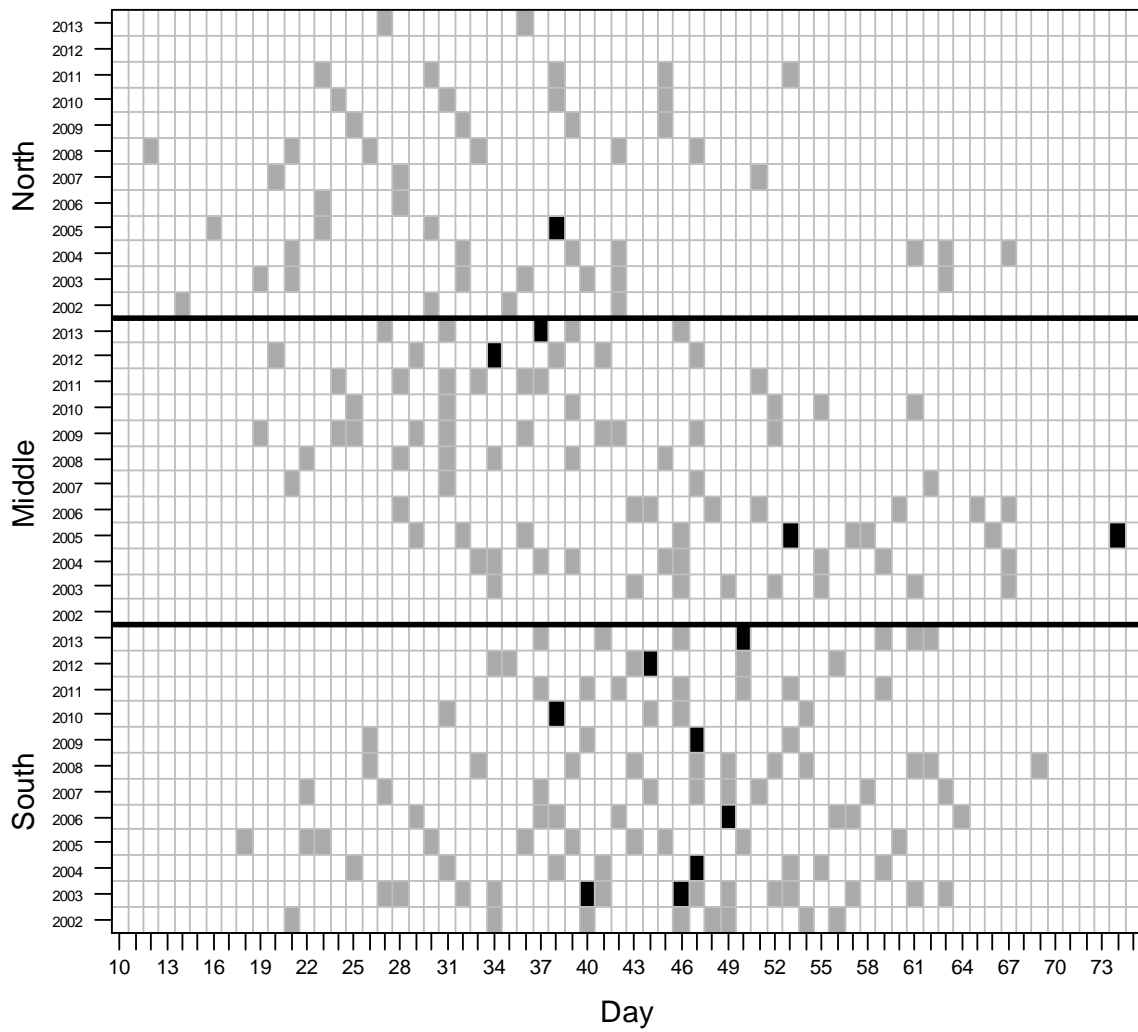


Figure 2. Number of experimental net samples per day (starting from August 1st) by region and year. Grey squares indicate one sample and black squares indicate that two fishermen were active.

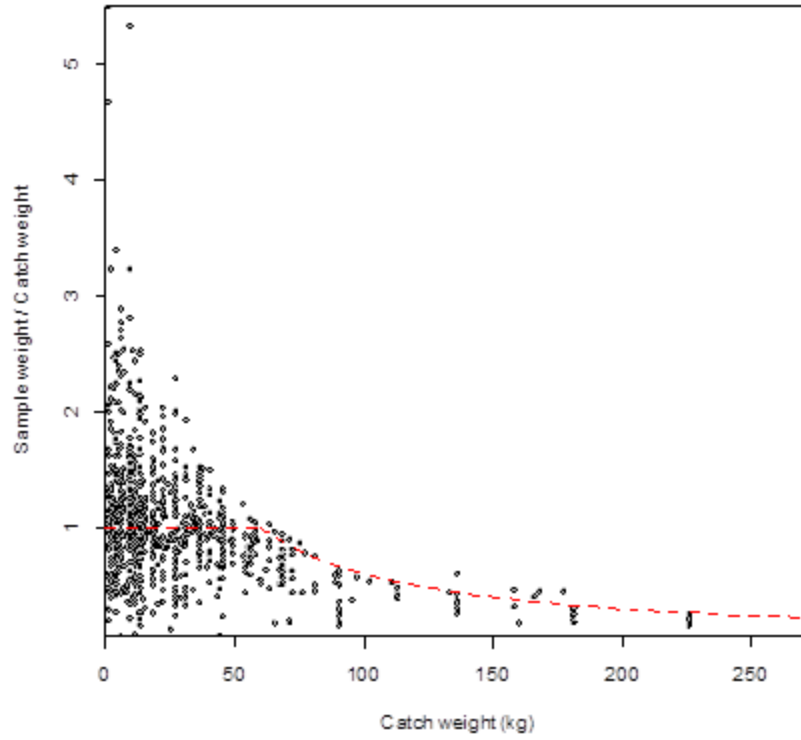


Figure 3. Ratio of sample weight to fisherman-estimated catch weight versus catch weight. The dashed line shows the theoretical sampling ratio under the prescribed fishing and sampling protocol.

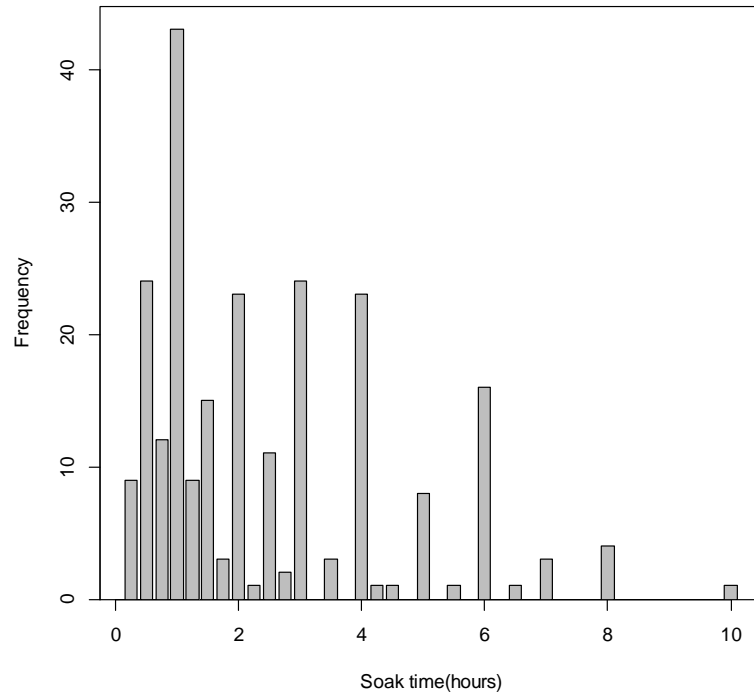


Figure 4. Histogram of reported experimental net soak times from logbooks.

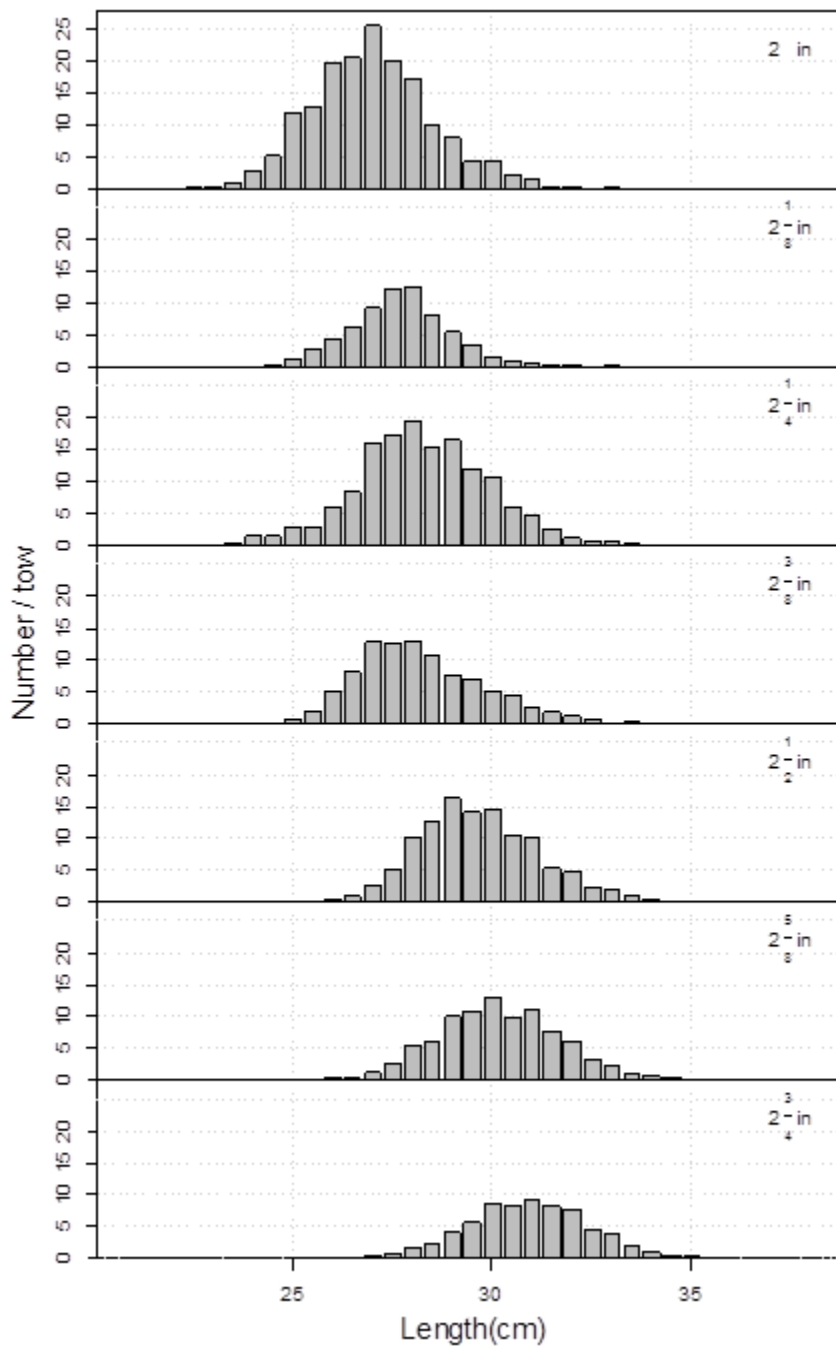


Figure 5. Mean number per standardized one-hour tow of samples averaged over years and regions.

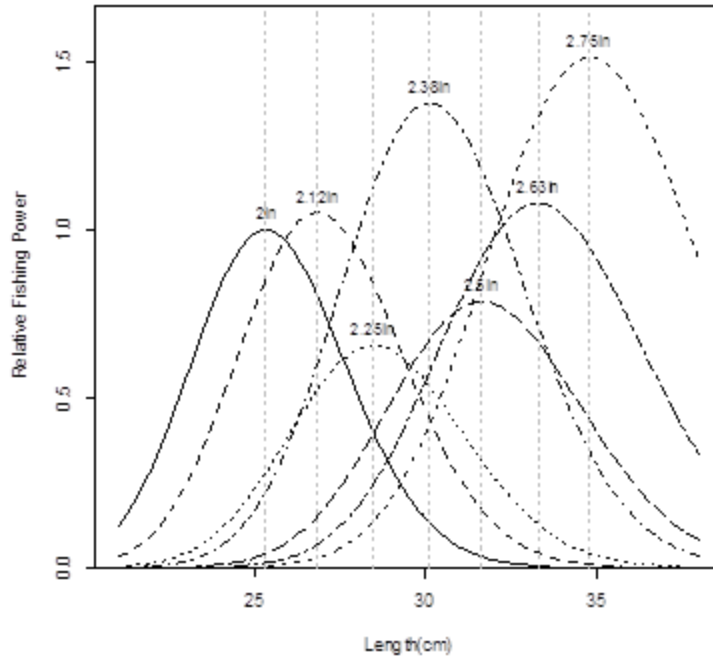


Figure 6. Estimated gamma-type selectivity curves for the variable-power, negative binomial model. The scales of the curves vary inconsistently with mesh size, as a monotone pattern would be expected.

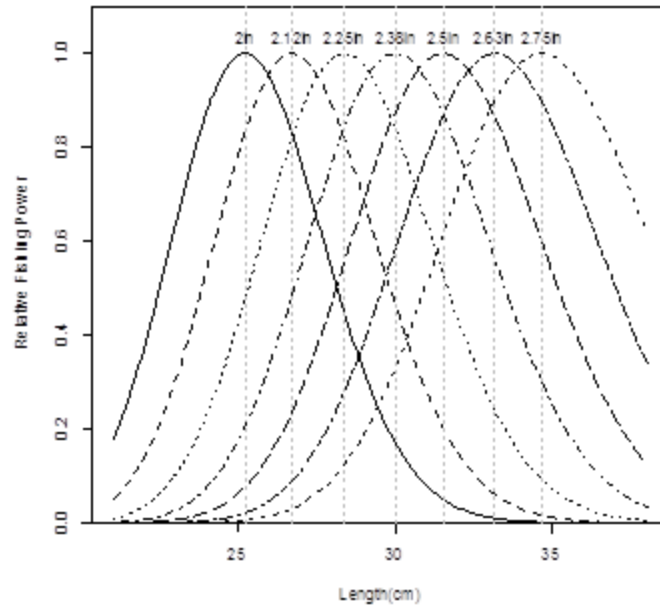


Figure 7. Fitted gamma-type selectivity curves by mesh size for the inference model based on the negative binomial with constant fishing power.

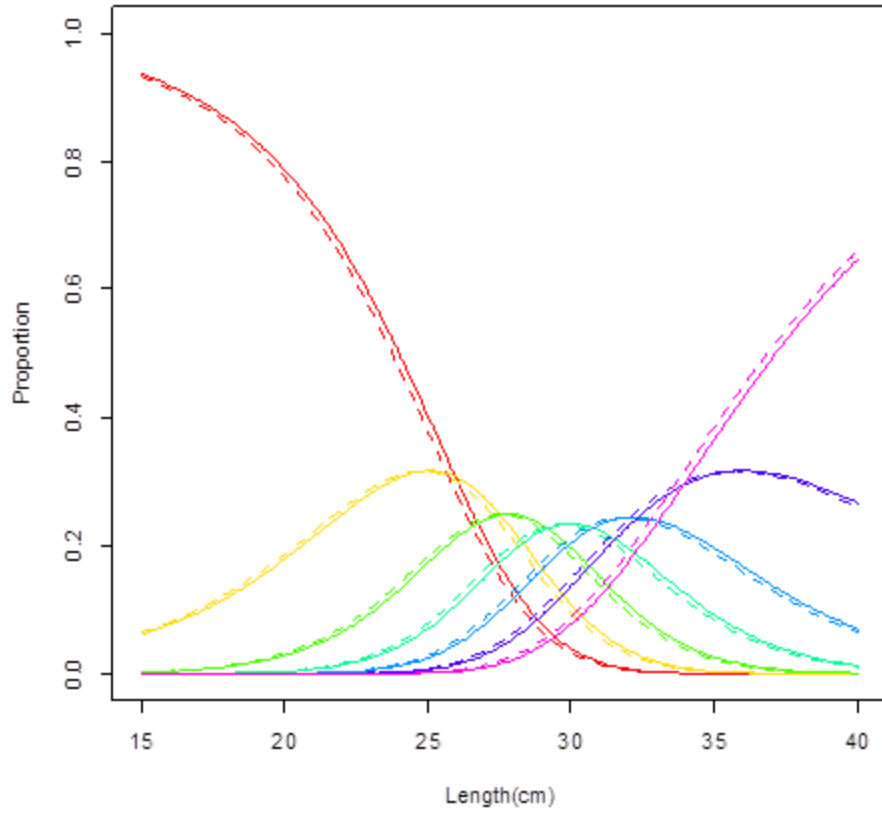


Figure 8. Proportions-at-length of Atlantic herring for each mesh size, as estimated from the inference model (solid line) and the model where fishing power of each panel is proportional to mesh size (dashed lines).

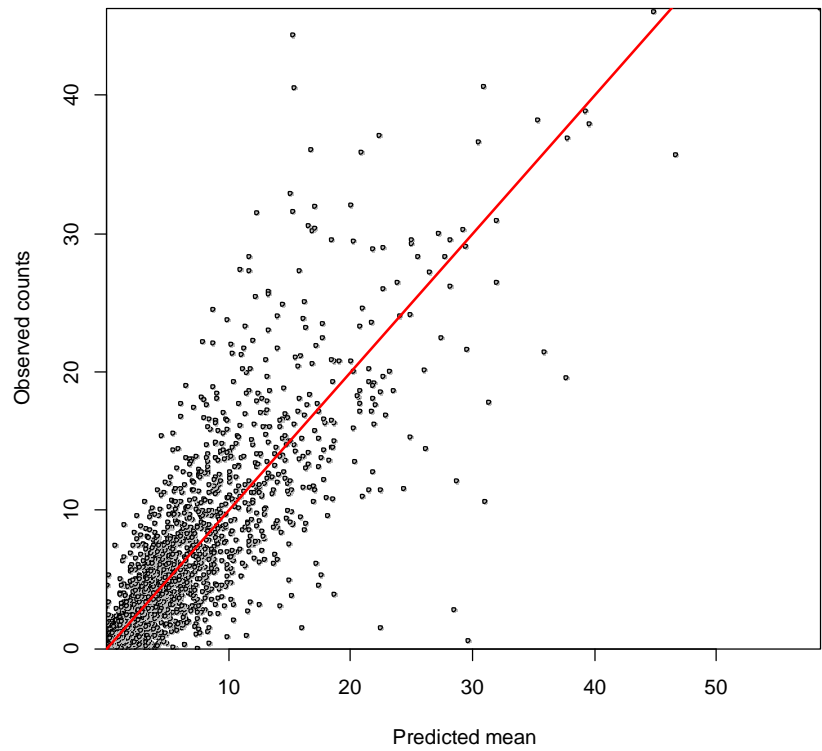


Figure 9. Standardized observed counts versus predicted mean counts from the inference model.

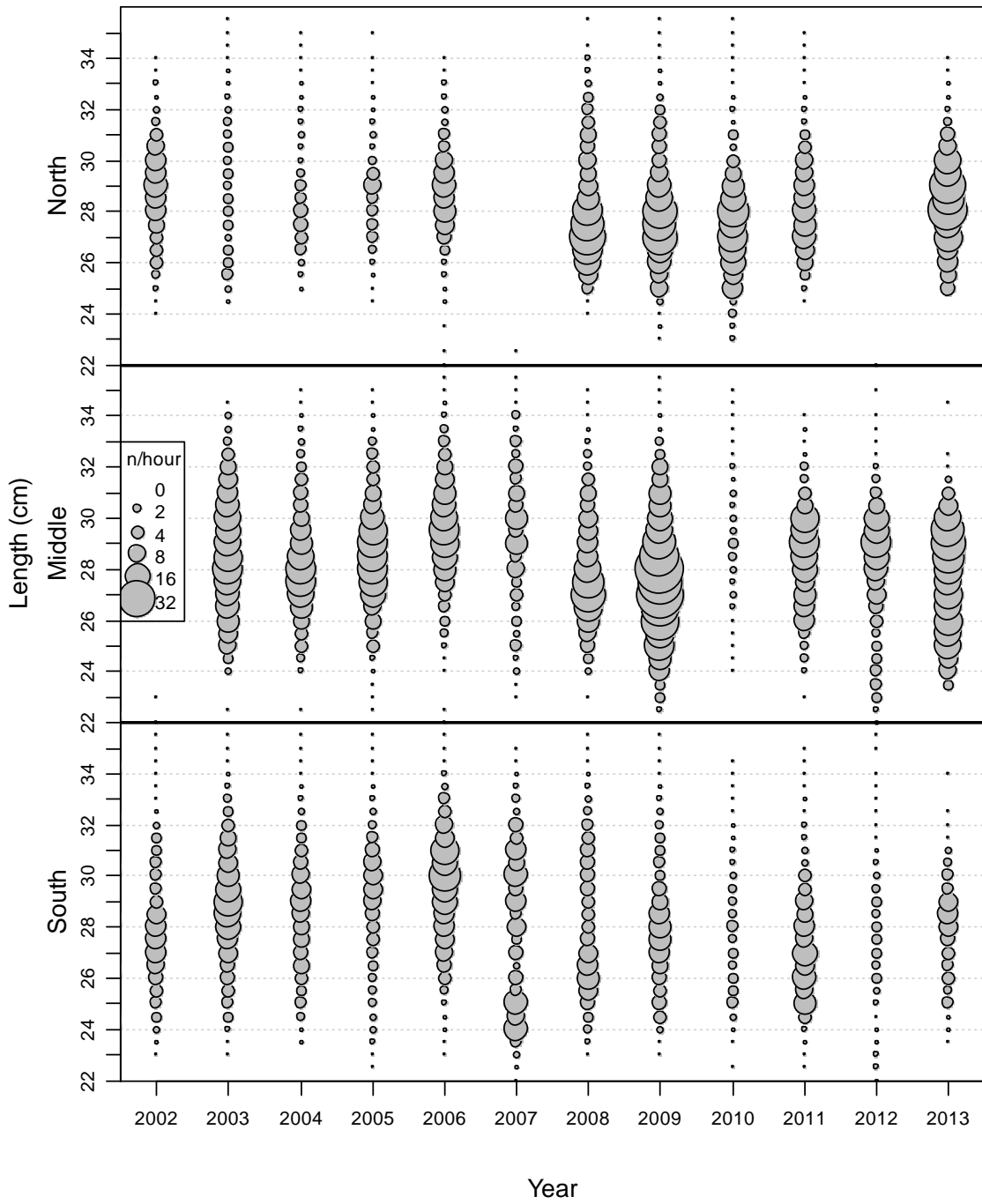


Figure 10. Catch-at-length index by year and region as inferred from the gillnet selectivity model. Circle areas are proportional to the estimated mean standardized catch, in numbers per hour.

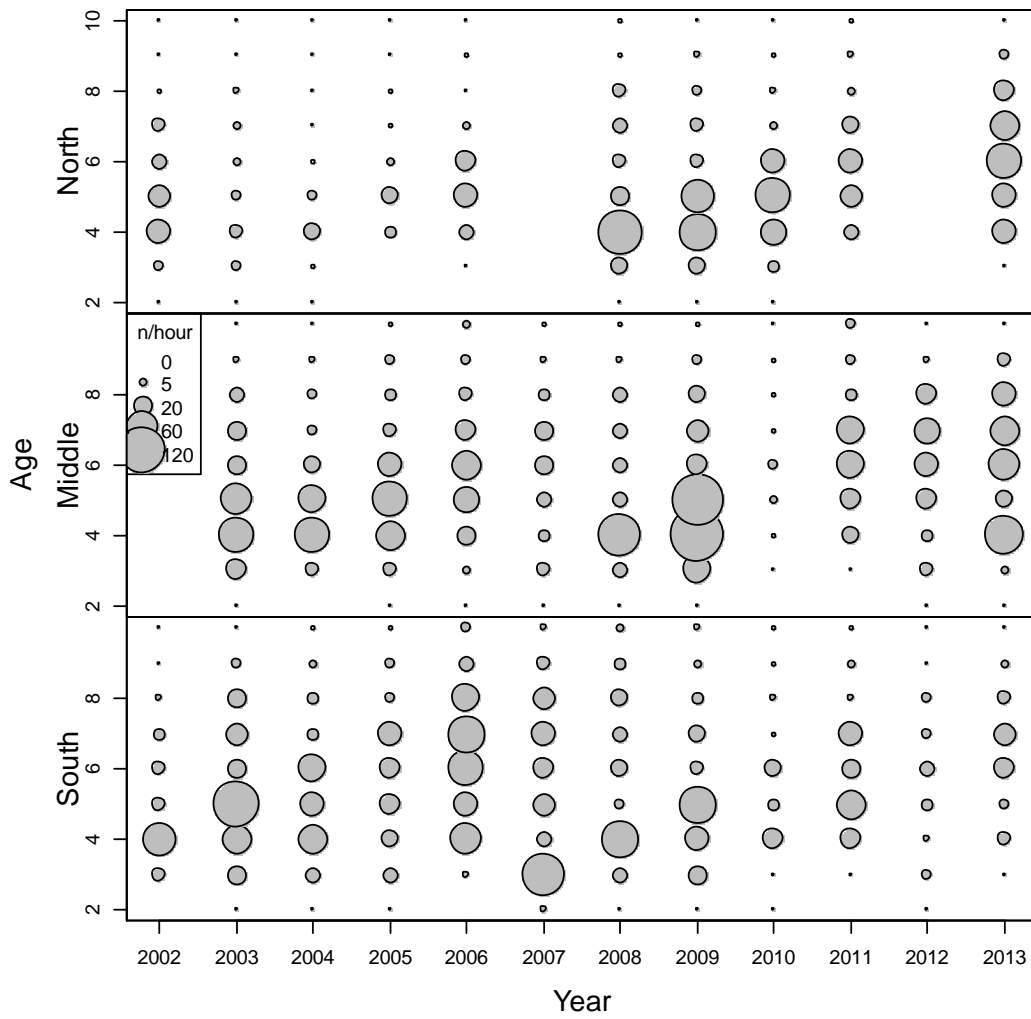


Figure 11. Bubble plot of catch-at-age estimates from the inference model by year and region. Circle areas are proportional to the estimated mean standardized catch, in numbers per hour.